



Topological superconducting phase and Majorana fermions in half-metal/superconductor heterostructures

Suk Bum Chung, Hai-Jun Zhang, Xiao-Liang Qi, and Shou-Cheng Zhang

Department of Physics, Stanford University, Stanford, California 94305, USA

(Received 19 July 2011; published 23 August 2011)

As a half-metal is spin polarized at its Fermi level by definition, it was conventionally thought to have little proximity effect to an s -wave superconductor. Here we show that with interface spin-orbit coupling $p_x + ip_y$ superconductivity without spin degeneracy is induced on the half-metal, and we give an estimate of its bulk energy gap. Therefore, a single-band half-metal can give us a topological superconductor with a single chiral Majorana edge state. Our band calculation shows that two atomic layers of VTe or CrO₂ is a single-band half-metal for a wide range (~ 0.1 eV) of Fermi energy and thus is a suitable candidate material.

DOI: [10.1103/PhysRevB.84.060510](https://doi.org/10.1103/PhysRevB.84.060510)

PACS number(s): 74.78.Fk, 71.10.Pm, 73.20.-r, 74.45.+c

Introduction. The possibility of Majorana fermions arising out of a condensed-matter system has aroused great interest in recent years.¹ One class of systems where Majorana fermions can appear is the two-dimensional (2D) chiral superconductor, which has a full pairing gap in the bulk, and \mathcal{N} gapless chiral one-dimensional (1D) states, which consists of Majorana fermions,^{2,3} at the edge. In a $\mathcal{N} = 1$ chiral topological superconductor (TSC), a single Majorana zero mode is bound to a vortex core,³⁻⁵ giving rise to non-Abelian statistics which can be potentially useful for topological quantum computation.⁶ The most straightforward way to realize such a chiral TSC is the intrinsic $p_x + ip_y$ superconductivity in spinless fermions.³ The strongest candidate material for this superconductivity, albeit a spinful version, is Sr₂RuO₄,⁷ but the experimental situation is not definitive.⁸ Recently, there have been alternative proposals involving inducing s -wave superconductivity in material with strong spin-orbit coupling through the proximity effect.⁹⁻¹⁷ It was pointed out in one of the proposals¹¹ that a spin-polarized $p_x + ip_y$ superconductor can be obtained in a ferromagnetic film through proximity to a superconductor. In this Rapid Communication, we further develop this approach and demonstrate through explicit calculations the feasibility of creating Majorana fermions in a half-metal/conventional s -wave superconductor heterostructure.

We consider the pair formation on a half-metal (HM) that is in proximity contact to an s -wave superconductor (SC). A HM, by definition, is spin polarized at the Fermi surface,¹⁸ i.e., it is a metal for the majority spin and an insulator for the minority spin. Our proposal has two major advantages over other current proposals. One is that our proposal does not require any fine tuning of the Fermi level. The other is that, due to better Fermi surface matching, we expect a more robust proximity effect between the SC and HM than between the SC and a semiconductor. It has been known that at the normal metal to s -wave SC interface, p -wave pairing can be induced due to broken inversion symmetry.¹⁹ Eschrig *et al.* showed that when normal metal is HM, even frequency pairing would be mostly p wave.²⁰ Furthermore, there are experimental indications of a strong proximity effect between a HM and an s -wave superconductor.^{21,22} Here we will show how we can obtain $p_x + ip_y$ pairing symmetry in a 2D HM when it is coupled to an s -wave superconductor only through electron hopping across the interface. (See Fig. 1.) If the 2D HM has a single

Fermi pocket without spin degeneracy, such $p_x + ip_y$ pairing will give us the TSC with $\mathcal{N} = 1$. We will show the band calculation for a thin-film material that is HM and has a single Fermi pocket. We will also discuss the suitable superconductor for optimizing this proximity effect and the method we can use for detecting the $p_x + ip_y$ pairing in the HM.

Basic model. We consider the model with a bulk s -wave superconductor and a 2D half-metal coupled by a weak hopping between two systems:

$$\mathcal{H} = \mathcal{H}_{\text{SC}} + \mathcal{H}_{\text{HM}} + \mathcal{H}_t, \quad (1)$$

where

$$\begin{aligned} \mathcal{H}_{\text{SC}} &= \sum_{\mathbf{k}, \sigma} (\epsilon'_{\mathbf{k}} - \mu') c_{\mathbf{k}\sigma}^\dagger c_{\mathbf{k}\sigma} + \sum_{\mathbf{k}} (\Delta'_{\mathbf{k}} c_{\mathbf{k}\uparrow}^\dagger c_{-\mathbf{k}\downarrow}^\dagger + \text{H.c.}), \\ \mathcal{H}_{\text{HM}} &= \sum_{\mathbf{k}_\parallel} (\epsilon_{\mathbf{k}_\parallel} - \mu) f_{\mathbf{k}_\parallel\uparrow}^\dagger f_{\mathbf{k}_\parallel\uparrow}, \\ \mathcal{H}_t &= \sum_{\mathbf{k}\sigma} (t_{\mathbf{k},\uparrow\sigma} f_{\mathbf{k}_\parallel\uparrow}^\dagger c_{\mathbf{k}\sigma} + \text{H.c.}); \end{aligned} \quad (2)$$

note that \mathbf{k}_\parallel is the in-plane projection of \mathbf{k} and the spin quantization axis is along the normal direction. This model provides a general mechanism for the SC proximity effect in the clean interface limit, where \mathbf{k}_\parallel is conserved in the hopping process. This model allows for both spin-conserving and spin-flip hopping. (See Figs. 1 and 2.)

In this model, the symmetry of the pairing correlation on the half-metal side $\langle f_{-\mathbf{k}_\parallel\uparrow} f_{\mathbf{k}_\parallel\uparrow} \rangle$ is determined entirely by $t_{\mathbf{k},\uparrow\sigma}$. In this model, the only channel for this Cooper-pair formation is to have the HM electrons with momenta \mathbf{k}_\parallel and $-\mathbf{k}_\parallel$ hop to the SC to form a pair there. This process requires that hopping flips the spin of either one of the \mathbf{k}_\parallel and $-\mathbf{k}_\parallel$ electrons. Since the Cooper pair on the SC side is in the spin-singlet s -wave state, the two processes interfere destructively, giving us

$$\langle f_{-\mathbf{k}_\parallel\uparrow} f_{\mathbf{k}_\parallel\uparrow} \rangle \propto t_{\mathbf{k}_\parallel,\uparrow\uparrow} t_{-\mathbf{k}_\parallel,\uparrow\downarrow} - t_{-\mathbf{k}_\parallel,\uparrow\uparrow} t_{\mathbf{k}_\parallel,\uparrow\downarrow}, \quad (3)$$

with an s -wave multiplicative factor when there is no k_\perp dependence; note the odd spatial parity. In the limit of weak hopping $|t_{\mathbf{k},\uparrow\sigma}| \ll |\Delta'_{\mathbf{k}}|$, we find the pairing amplitude at the HM Fermi surface (where $\epsilon_{\mathbf{k}_\parallel} = \mu$) to be²³

$$\langle f_{-\mathbf{k}_\parallel\uparrow} f_{\mathbf{k}_\parallel\uparrow} \rangle \approx \frac{1}{2} \left\langle \frac{\eta_{\mathbf{k}}}{\sqrt{|\eta_{\mathbf{k}}|^2 + |\zeta_{\mathbf{k}}|^2}} \right\rangle_{k_\perp}, \quad (4)$$

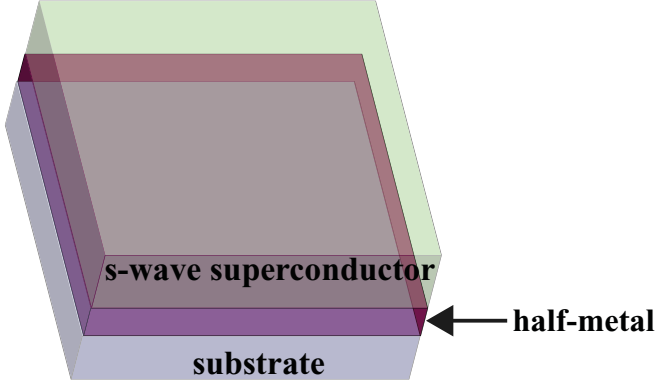


FIG. 1. (Color online) The heterostructure for obtaining $p_x + ip_y$ superconductivity. The half-metal layer has a 2D electronic structure with a single Fermi surface without spin degeneracy. It is coupled to the s -wave superconductor through hopping. The substrate stabilizes the half-metal crystal structure without affecting qualitatively its electronic structure.

where $\mathbf{k} = (\mathbf{k}_{\parallel}, k_{\perp})$, $\langle \dots \rangle_{k_{\perp}}$ is averaging over k_{\perp} , and

$$\begin{aligned} \eta_{\mathbf{k}} &= (t_{\mathbf{k},\uparrow\uparrow}t_{-\mathbf{k},\uparrow\downarrow} - t_{\mathbf{k},\uparrow\downarrow}t_{-\mathbf{k},\uparrow\uparrow})(c_{-\mathbf{k}\downarrow}c_{\mathbf{k}\uparrow})|_{\epsilon_{\mathbf{k}_{\parallel}}=\mu}, \\ \zeta_{\mathbf{k}} &= \frac{|t_{\mathbf{k},\uparrow\uparrow}|^2 + |t_{\mathbf{k},\uparrow\downarrow}|^2}{2} [(\epsilon'_{\mathbf{k}} - \mu')/E'_{\mathbf{k}}]_{\epsilon_{\mathbf{k}_{\parallel}}=\mu}, \end{aligned} \quad (5)$$

with $E'_{\mathbf{k}} = \sqrt{(\epsilon'_{\mathbf{k}} - \mu')^2 + |\Delta'_{\mathbf{k}}|^2}$ ($|t_{\mathbf{k},\uparrow\sigma}|^2 = |t_{-\mathbf{k},\uparrow\sigma}|^2$ assumed). Equations (4) and (5) tell us that if the Fermi surfaces of the HM and the SC match exactly for all values of k_{\perp} (i.e., $\epsilon'_{\mathbf{k}} = \mu'$ when $\epsilon_{\mathbf{k}_{\parallel}} = \mu$), we have $\langle f_{-\mathbf{k}_{\parallel}\uparrow} f_{\mathbf{k}_{\parallel}\uparrow} \rangle = e^{i\phi_{\mathbf{k}}} \langle c_{-\mathbf{k}\downarrow} c_{\mathbf{k}\uparrow} \rangle$ at the HM Fermi surface, with $e^{i\phi_{\mathbf{k}}}$ being the phase factor of $t_{\mathbf{k},\uparrow\uparrow}t_{-\mathbf{k},\uparrow\downarrow} - t_{\mathbf{k},\uparrow\downarrow}t_{-\mathbf{k},\uparrow\uparrow}$. Physically, $\eta_{\mathbf{k}}$ is proportional to the amplitude that the \mathbf{k}_{\parallel} and $-\mathbf{k}_{\parallel}$ HM electrons hop to the s -wave SC with opposite spins and form a Cooper pair, while $\zeta_{\mathbf{k}}$ is proportional to the amplitude that these electrons hop to the SC with their spins aligned and do not form a Cooper pair.

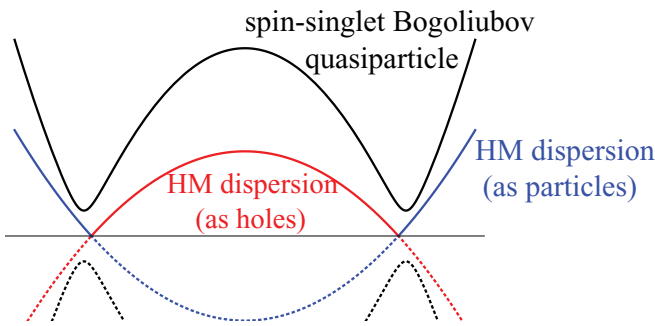


FIG. 2. (Color online) A schematic representation of the HM and SC bands for weak hopping. Two HM bands are due to the artificial doubling of degrees of freedom in the Bogoliubov-de Gennes formalism. In this formalism, the pairing amplitude and gap require hybridization of the “particle” and “hole” bands, which is due to the interface hopping in our model.

Our model gives us not only the pairing amplitude but also the pairing gap on the HM side. In the weak hopping limit we have been discussing, we obtain

$$\Delta_{\mathbf{k}}^{\text{HM}} = \left\langle \frac{\eta_{\mathbf{k}}}{E'_{\mathbf{k}}} \right\rangle_{k_{\perp}} = \left\langle \frac{t_{\mathbf{k},\uparrow\uparrow}t_{-\mathbf{k},\uparrow\downarrow} - t_{\mathbf{k},\uparrow\downarrow}t_{-\mathbf{k},\uparrow\uparrow}}{2E_{\mathbf{k}}'^2} \Delta'_{\mathbf{k}} \right\rangle_{k_{\perp}} \quad (6)$$

at the HM Fermi surface.²³ Note here that $|\Delta'_{\mathbf{k}}|$ is maximized when we have a perfect Fermi surface matching between the HM and the SC. Equation (6) tells us that we have an energy gap in the HM due to the proximity induced electron pairing of Eq. (4) because the HM is in the 2D limit.^{24,25} Therefore, the topological property of SC induced in the HM is determined entirely by $t_{\mathbf{k},\uparrow\sigma}$.

In the limit of strong hopping, we obtain a much larger pairing gap while Eq. (3) still holds. Our strong hopping limit requires that, at the HM Fermi surface, the energetics is dominated by the spin-conserving hopping $t_{\mathbf{k},\uparrow\uparrow}$, i.e., $|t_{\mathbf{k},\uparrow\uparrow}| \gg E'_{\mathbf{k}}$ and $|t_{\mathbf{k},\uparrow\uparrow}| \gg |t_{\mathbf{k},\uparrow\downarrow}|$. Within this model, at the HM Fermi surface, the pairing amplitude is still given by Eq. (4), while the pairing gap now²³

$$\Delta_{\mathbf{k}}^{\text{HM}} = \left\langle \frac{\eta_{\mathbf{k}} E'_{\mathbf{k}}}{|t_{\mathbf{k},\uparrow\uparrow}|^2} \right\rangle_{k_{\perp}} = \left\langle \frac{t_{\mathbf{k},\uparrow\uparrow}t_{-\mathbf{k},\uparrow\downarrow} - t_{\mathbf{k},\uparrow\downarrow}t_{-\mathbf{k},\uparrow\uparrow}}{2|t_{\mathbf{k},\uparrow\uparrow}|^2} \Delta'_{\mathbf{k}} \right\rangle_{k_{\perp}}. \quad (7)$$

The above HM pairing gap is much larger than that of Eq. (6); note that in Eq. (7) Δ^{HM} is proportional to $t_{\uparrow\downarrow}/t_{\uparrow\uparrow}$, while in Eq. (6) it is proportional to $t_{\uparrow\downarrow}t_{\uparrow\uparrow}/E'^2$.

Interface hopping. To show how the $p_x + ip_y$ pairing arises in this proximity effect, we first discuss the interface spin-orbit coupling (SOC) giving a chiral \mathbf{k}_{\parallel} -odd contribution to $t_{\mathbf{k},\uparrow\downarrow}$. We note that, at the bulk HM/bulk SC interface, there is Rashba SOC due to broken inversion symmetry^{11,19}: $\mathcal{H}_{\text{SOC}} = \hbar\alpha(\boldsymbol{\sigma} \times \mathbf{k}) \cdot \hat{\mathbf{n}}\delta(\hat{\mathbf{n}} \cdot \mathbf{r})$, where $\hat{\mathbf{n}}$ is the interface normal. The analog of this SOC in our model should be contained in \mathcal{H}_t , as it affects only electrons whose wave functions extend across the interface. Also, it should contribute to spin-flip hopping for nonzero \mathbf{k}_{\parallel} , as the HM is spin polarized along the interface normal. Such a hopping term, with the symmetry of the Rashba SOC, needs to be in the form

$$\mathcal{H}_{t\text{-SOC}} = t_{\text{SOC}} \sum_{\mathbf{k}} F_{\mathbf{k}_{\parallel}}^{\dagger} (\sigma^x \sin k_y a - \sigma^y \sin k_x a) C_{\mathbf{k}} + \text{H.c.}, \quad (8)$$

where $F_{\mathbf{k}} = (f_{\mathbf{k}_{\parallel}\uparrow}, f_{\mathbf{k}_{\parallel}\downarrow})^T$ and $C_{\mathbf{k}} = (c_{\mathbf{k}\uparrow}, c_{\mathbf{k}\downarrow})^T$. However, the terms involving $f_{\mathbf{k}_{\parallel}\downarrow}$ can be projected out due to the HM minority-spin gap, leaving only the $t_{\mathbf{k},\uparrow\downarrow}$ term.

We can now show explicitly how we obtain the $p_x + ip_y$ pairing from $t_{\mathbf{k},\uparrow\sigma}$. For this we take the $t_{\mathbf{k},\uparrow\downarrow}$ obtained above and set $t_{\mathbf{k},\uparrow\uparrow}$ to be momentum independent:

$$t_{\mathbf{k},\uparrow\uparrow} = t_0, \quad (9)$$

$$t_{\mathbf{k},\uparrow\downarrow} = t_{\text{SOC}}(i \sin k_x a + \sin k_y a).$$

Inserting this into Eq. (3) gives us the chiral p -wave pairing on the HM side:

$$\begin{aligned} \langle f_{-\mathbf{k}_{\parallel}\uparrow} f_{\mathbf{k}_{\parallel}\uparrow} \rangle &\propto t_{\mathbf{k}_{\parallel},\uparrow\uparrow}t_{-\mathbf{k}_{\parallel},\uparrow\downarrow} - t_{-\mathbf{k}_{\parallel},\uparrow\uparrow}t_{\mathbf{k}_{\parallel},\uparrow\downarrow} \\ &= -2it_0 t_{\text{SOC}}(\sin k_x a - i \sin k_y a). \end{aligned} \quad (10)$$

We can see from the real-space representation that Eq. (9) is a physically reasonable hopping. Assuming that the HM

electrons can hop only to the top layer of the SC and we have a square lattice, the dominant hopping is the $t_{\mathbf{k},\uparrow\uparrow}$ of Eq. (9): $t_0 \sum_i f_{i\uparrow}^\dagger c_{i\uparrow} + \text{H.c.}$ Therefore, the pairing symmetry Eq. (3) will be determined by the largest spin-flip hopping with odd spatial symmetry, and that should of the “nearest-neighbor” type, i.e., $\sum_{\delta\mathbf{r}_{\parallel}/a=\pm\hat{x},\pm\hat{y}} t_{\delta\mathbf{r}_{\parallel}} f_{i\uparrow}^\dagger c_{i+\delta\mathbf{r}_{\parallel},\downarrow} + \text{H.c.}$, where $t_{-\delta\mathbf{r}} = -t_{\delta\mathbf{r}}$. This hopping can be expressed as a sum of the Rashba-like $t_{\mathbf{k},\uparrow\downarrow}$ of Eq. (9), and of a Dresselhaus-like term; however, the chirality of Eq. (10) is maintained unless the Dresselhaus-like and the Rashba-like terms are equal in magnitude. Therefore, the topological property of this p -wave pairing is robust against any small modification to the hopping term. Equation (9) gives us the $\mathcal{N} = 1$ TSC in the strong hopping limit as well as the weak hopping limit.²³ We also note that the $p_x + ip_y$ is considered to be the likely pairing symmetry for intrinsic SC in a HM.²⁹

From the origin of the interface SOC, we can estimate of the HM pairing gap to be

$$|\Delta^{\text{HM}}| \sim |\Delta'|(\alpha_{\text{SOC}}/W), \quad (11)$$

where α_{SOC} is the Rashba SOC of the s -wave SC and W is the bandwidth. Physically, when SOC is strong for the s -wave SC but weak for the HM, we can expect to have the interface SOC. This situation is experimentally relevant because s -wave SC can exist in materials with strong SOC, while the spin-polarized angle-resolved photoemission spectroscopy (ARPES) indicates complete spin polarization for the HM, as in CrO_2 .³⁰ Assuming that we have zero effective SOC on the HM, we will effectively have the spin-orbit coupling hopping $t_{\text{SOC}} \sim (\alpha_{\text{SOC}}/W)t_0$ induced through second-order perturbation. This is sufficient for estimating $|\Delta^{\text{HM}}|$, because, in the strong hopping limit, we find $\Delta^{\text{HM}} \sim (t_{\text{SOC}}/t_0)\Delta'$ by inserting Eq. (10) into Eq. (7).

We also point out that this HM/SC proximity effect can provide us with a means to obtain a multidomain chiral p -wave SC. Equations (8) and (9) show us that if we reverse the HM spin polarization, then we will also reverse the chirality of the induced SC. Therefore, in a HM, a domain boundary between opposite spin polarization will also be the domain boundary between the $p_x + ip_y$ and $p_x - ip_y$ domain when SC is induced.

Candidate material. We note that the spin-polarized (or single-spin) $p_x + ip_y$ SC with a single Fermi pocket gives us the $\mathcal{N} = 1$ TSC,³ but the same cannot be said for the $p_x + ip_y$ SC with multiple Fermi pockets.^{31,32} Therefore, to obtain the $\mathcal{N} = 1$ TSC, it is important that we find a 2D HM with a single Fermi pocket, as we have in Eq. (2). That way, the HM/SC proximity effect we discussed will give us an equivalent of the single-spin $p_x + ip_y$ SC with a single Fermi pocket. However, applying the Luttinger theorem to HM tells us that, in order to have a single Fermi pocket, we need a fractional number of electrons per unit cell.

One candidate material for a 2D HM with a single Fermi pocket is zinc-blende VTe or CrTe that is two atomic layers thick in the (111) direction. (See Fig. 3 for the lattice structure.) We identified candidate material through *ab initio* band calculations performed in the frame of density functional theory^{33,34} with the plane-wave pseudopotential method.²³ Both VTe and CrTe in the zinc-blende structure have been

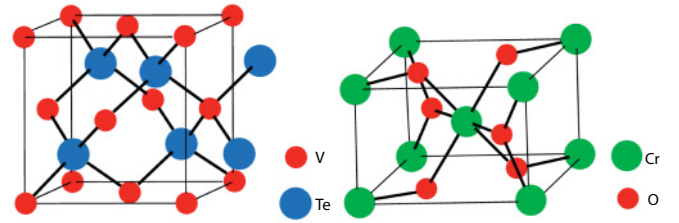


FIG. 3. (Color online) Crystal structures of two candidate materials, VTe and CrO_2 . The left-hand side shows the zinc-blende crystal structure of bulk VTe. Here, both V and Te forms are body-centered cubic with a lattice constant of $a = 0.6271$ nm ($a = 0.6202$ nm for zb-CrTe). The right-hand side shows the rutile crystal structure of bulk CrO_2 , where $a = 0.4421$ nm, $c = 0.2916$ nm. The distance between the nearest O and Cr on the same layer is 0.1817 nm.

shown to be HM in the band calculation;³⁵ a thin film of the zinc-blende CrTe has been fabricated in thin films by molecular beam epitaxy.³⁶ As we see in Fig. 4, two atomic layers of zinc-blende VTe (111) on the zinc-blende ZnTe substrate is a single Fermi pocket HM at 0 eV. This is due to a charge-transfer mechanism²³ that gives us one-half electrons per unit cell; there are analogous previous examples.^{37,38} As we have a 0.3-eV range for the Fermi level that gives us a single Fermi pocket, unlike in many of the previous proposals for obtaining the $\mathcal{N} = 1$ TSC (Ref. 12) we do not require fine

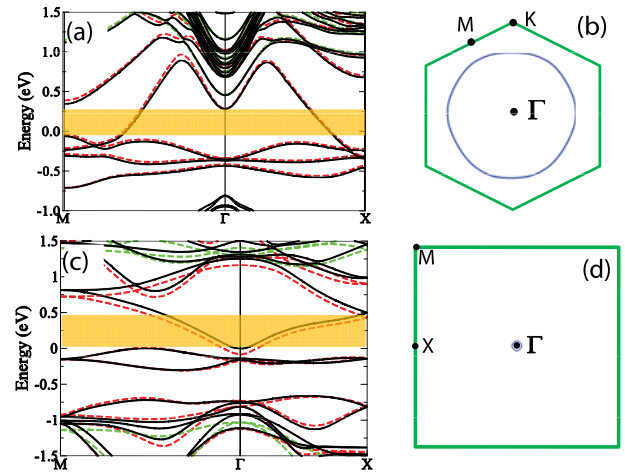


FIG. 4. (Color online) (a) The band structure of the VTe-ZnTe(111) model. There is no spin degeneracy in these bands; the red (darker gray) and the green (gray) dotted curve shows the spin-up and spin-down bands when SOC is absent. The region shaded in orange (lighter gray) shows the energy range for which we obtain a single Fermi pocket. (b) The single Fermi surface at the energy level 0.0 eV for the ZnTe-VTe(111) model. The green (gray) box shows the first Brillouin zone (BZ). (c) The band structure of the CrO_2 (001) model. (d) The single Fermi surface around the Γ point at the energy level 0.01 eV for the CrO_2 (001) model, the green (gray) box showing the first BZ.

tuning of the HM Fermi level. CrTe has a single Fermi pocket for a narrower Fermi-level range (≈ 0.06 eV).

We also point out that the CrO₂ film that is two atomic layers thick in the (001) direction comes close to fulfilling our requirement. Bulk CrO₂ has been experimentally confirmed to be HM,^{30,39} and it was also shown in the experiment to have a strong proximity effect to an *s*-wave SC—NbTiN—that has a relatively high T_c (~ 14 K) and a spin-orbit coupling that is larger than the SC gap. Since the width of the bands near the Fermi level for NbN is ~ 7.2 eV (Ref. 40) and the atomic spin-orbit coupling of Nb is 0.1 eV,⁴¹ a pairing gap up to ~ 1 K can be estimated from Eq. (11). The bulk CrO₂ crystal, as shown in Fig. 4, has a rutile structure.⁴² The band calculation for two atomic layers of CrO₂ (001) in a perfect rutile structure gives us a single Fermi pocket HM when we raise the Fermi level by 0.01 eV (although at 0 eV there are additional Fermi pockets).²³ For a Fermi-level range of ~ 0.5 eV, this material is a single Fermi pocket HM.

Detection. Detecting a single chiral Majorana edge state along with the fully gapped quasiparticle spectrum in the bulk of the HM will confirm that we have $\mathcal{N} = 1$ TSC in the HM. When a large enough $|\Delta^{\text{HM}}|$, one direct method would be to

detect with scanning tunneling microscopy (STM) a zero-bias peak only at the edge or along the HM domain boundary.^{22,43} The chiral Majorana state can also be detected from transport experiments.^{44,45}

In summary, we have shown that we can obtain the $\mathcal{N} = 1$ TSC in a HM through a proximity effect with an *s*-wave SC. In a model where the HM is coupled to the SC through hopping, the symmetry of SC pairing induced in the HM is determined entirely by the hopping term. Due to the interface Rashba spin-orbit coupling, the hopping term will induce the pairing with $p + ip$ symmetry. In order for this $p_x + ip_y$ pairing to lead to the $\mathcal{N} = 1$ TSC, we need to have a HM with a single Fermi surface, and our band calculation shows that this can be obtained for a very thin CrO₂ film. STM measurements can be used to verify that TSC is induced in the HM.

We would like to thank Mac Beasley, Richard Martin, and Patrick Lee for sharing their insights; we also acknowledge helpful discussions with Steve Kivelson, Srinivas Raghu, and Kookrin Char. This work is supported by DOE under Contract No. DE-AC02-76SF00515 (S.B.C.), the Sloan Foundation (X.L.Q.), and NSF under Grant No. DMR-0904264.

-
- ¹F. Wilczek, *Nat. Phys.* **5**, 614 (2009).
²G. E. Volovik, *Sov. Phys. JETP* **67**, 1804 (1988).
³N. Read and D. Green, *Phys. Rev. B* **61**, 10267 (2000).
⁴R. Jackiw and P. Rossi, *Nucl. Phys. B* **190**, 681 (1981).
⁵G. E. Volovik, *JETP Lett.* **70**, 609 (1999).
⁶C. Nayak, S. H. Simon, A. Stern, M. Freedman, and S. Das Sarma, *Rev. Mod. Phys.* **80**, 1083 (2008).
⁷A. P. Mackenzie and Y. Maeno, *Rev. Mod. Phys.* **75**, 657 (2003).
⁸P. G. Bjornsson, Y. Maeno, M. E. Huber, and K. A. Moler, *Phys. Rev. B* **72**, 012504 (2005); J. Kirtley *et al.*, *ibid.* **76**, 014526 (2007).
⁹L. Fu and C. L. Kane, *Phys. Rev. Lett.* **100**, 096407 (2008).
¹⁰M. Sato and S. Fujimoto, *Phys. Rev. B* **79**, 094504 (2009).
¹¹P. A. Lee, e-print [arXiv:0907.2681](http://arxiv.org/abs/0907.2681).
¹²J. D. Sau, R. M. Lutchyn, S. Tewari, and S. Das Sarma, *Phys. Rev. Lett.* **104**, 040502 (2010).
¹³X.-L. Qi, T. L. Hughes, and S.-C. Zhang, *Phys. Rev. B* **82**, 184516 (2010).
¹⁴R. M. Lutchyn, J. D. Sau, and S. Das Sarma, *Phys. Rev. Lett.* **105**, 077001 (2010).
¹⁵J. Alicea, *Phys. Rev. B* **81**, 125318 (2010).
¹⁶Y. Oreg, G. Refael, and F. von Oppen, *Phys. Rev. Lett.* **105**, 177002 (2010).
¹⁷M. Duckheim and P. W. Brouwer, *Phys. Rev. B* **83**, 054513 (2011).
¹⁸R. A. de Groot, F. M. Mueller, P. G. van Engen, and K. H. J. Buschow, *Phys. Rev. Lett.* **50**, 2024 (1983).
¹⁹L. P. Gor'kov and E. I. Rashba, *Phys. Rev. Lett.* **87**, 037004 (2001); V. M. Edelstein, *Phys. Rev. B* **67**, 020505 (2003).
²⁰M. Eschrig, J. Kopu, J. C. Cuevas, and G. Schön, *Phys. Rev. Lett.* **90**, 137003 (2003).
²¹R. S. Keizer *et al.*, *Nature (London)* **439**, 825 (2006).
²²Y. Kalcheim, T. Kirzhner, G. Koren, and O. Millo, *Phys. Rev. B* **83**, 064510 (2011).
²³See Supplemental Materials at <http://link.aps.org/supplemental/10.1103/PhysRevB.84.060510> for derivations and details.
²⁴G. Deutscher, *Rev. Mod. Phys.* **77**, 109 (2005).
²⁵Although electron-electron interaction in the HM can modify this gap (Ref. 26), good agreement between the CrO₂ specific heat obtained from band calculation (Ref. 27) and experiment (Ref. 28) indicates that the interaction effect can be small in HM.
²⁶P. G. de Gennes, *Rev. Mod. Phys.* **36**, 225 (1964).
²⁷I. I. Mazin, D. J. Singh, and C. Ambrosch-Draxl, *J. Appl. Phys.* **85**, 6220 (1999).
²⁸H. Liu *et al.*, *Phys. Status Solidi A* **202**, 144 (2005).
²⁹W. E. Pickett, *Phys. Rev. Lett.* **77**, 3185 (1996).
³⁰Yu. S. Dedkov *et al.*, *Appl. Phys. Lett.* **80**, 4181 (2002).
³¹S. Raghu, A. Kapitulnik, and S. A. Kivelson, *Phys. Rev. Lett.* **105**, 136401 (2010).
³²X.-L. Qi, T. L. Hughes, and S.-C. Zhang, *Phys. Rev. B* **81**, 134508 (2010).
³³P. Hohenberg and W. Kohn, *Phys. Rev.* **136**, B864 (1964).
³⁴W. Kohn and L. J. Sham, *Phys. Rev.* **140**, A1133 (1965).
³⁵W.-H. Xie, Y.-Q. Xu, B.-G. Liu, and D. G. Pettifor, *Phys. Rev. Lett.* **91**, 037204 (2003).
³⁶M. G. Sreenivasan, J. F. Bi, K. L. Teo, and T. Liew, *J. Appl. Phys.* **103**, 043908 (2008).
³⁷W. A. Harrison, E. A. Kraut, J. R. Waldrop, and R. W. Grant, *Phys. Rev. B* **18**, 4402 (1978).
³⁸Z. S. Popovic, S. Satpathy, and R. M. Martin, *Phys. Rev. Lett.* **101**, 256801 (2008).
³⁹R. J. Soulen *et al.*, *Science* **282**, 85 (1998).
⁴⁰L. F. Mattheiss, *Phys. Rev. B* **5**, 315 (1972).
⁴¹D. Machin and J. Sullivan, *J. Less Common Met.* **19**, 405 (1969).
⁴²M. A. Korotin, V. I. Anisimov, D. I. Khomskii, and G. A. Sawatzky, *Phys. Rev. Lett.* **80**, 4305 (1998).
⁴³M. Yamashiro, Y. Tanaka, and S. Kashiwaya, *Phys. Rev. B* **56**, 7847 (1997).
⁴⁴I. Serban, B. Béni, A. R. Akhmerov, and C. W. J. Beenakker, *Phys. Rev. Lett.* **104**, 147001 (2010).
⁴⁵S. B. Chung, X.-L. Qi, J. Maciejko, and S.-C. Zhang, *Phys. Rev. B* **83**, 100512 (2011).